airgap. It has been derived on the basis of the following assumptions: (*a*) all r.f. quantities vary as exp $[i(\omega t \mp ky)]$ and are z-independent, where ω is the angular frequency and k is the complex wavenumber, (*b*) the mechanical motion is linearly polarised in the z-direction, i.e. horizontally polarised shear, (*c*) the exchange effect is neglected, (*d*) the effects of generation, recombination and trapping of carriers is neglected and (*e*) quasistatic approximation is made. The drift velocity v_d is taken as positive in the same direction of propagation.

We shall confine ourselves to $-y$ directed m.e.l.w.s in the following, since $+y$ directed m.e.l.w.s are not coupled with m.s.s.w.s for the biasing case as in Fig 1,[4,5] i e. in Fig 1, m.s.s.w.s propagate in only the $-y$ direction.

We have computed the drift-velocity dependence of the amplification coefficient of m.e.l.w.s taking the carrier concentration n_0 as a parameter. The gain per unit length α is calculated from $\alpha = (20 \log e)(Im\, k)$ dB/m. The numerical results are presented graphically in Figs. 2 and 3 for a system that consists of zinc oxide ($d = 1$ μm), gallium-y.i.g. (saturation magnetisation $\mu_0 M = 300$ gauss) and n-type germanium.

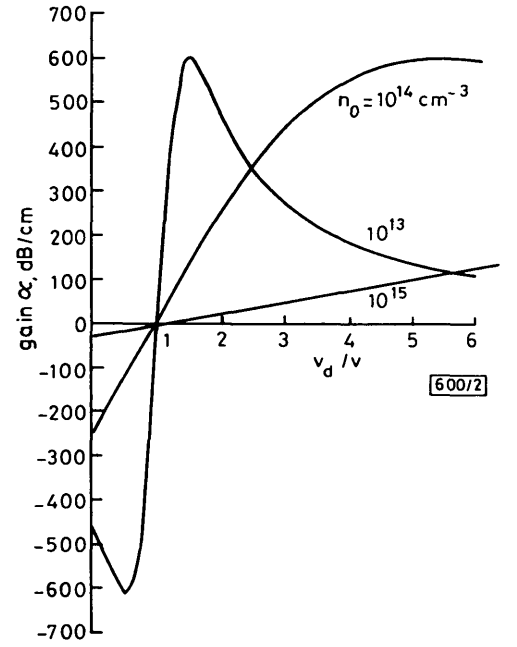

Fig. 2 *Amplification characteristics of m.e.l.w.s by interaction with carrier waves when diffusion neglected*

The layered composite consists of zinc oxide, gallium-y.i.g. ($\mu_0 M = 300$ gauss), and n-type germanium. Layer thickness $d = 1$ μm, frequency $\omega/2\pi = 984$ MHz and magnetic field $B_0 = 50$ gauss

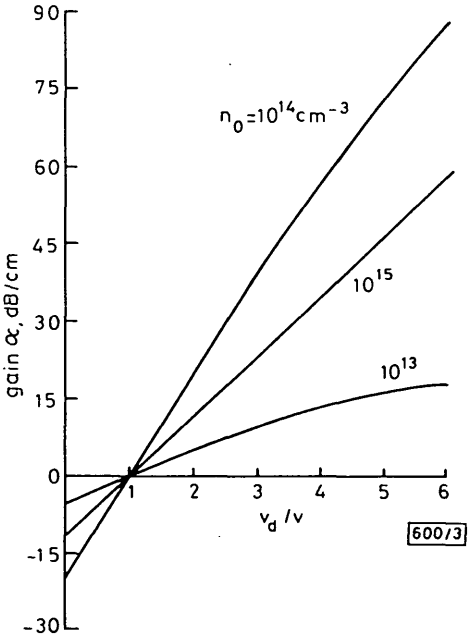

Fig. 3 *Amplification characteristics of m.e.l.w.s when diffusion included*

The layered composite is the same as Fig. 2

In the present calculations it was assumed that at room temperature $B_0 = 50$ gauss and $\omega/2\pi = 984$ MHz. This frequency is slightly higher than the higher limit of ferrite-metal mode propagation of m.s.s.w.s in the substrate and lies in the region of the magnetoelastic coupling. At this frequency the phase velocity v of m.e.l.w.s is $\approx 3{\cdot}3 \times 10^3$ m/s. The phase velocity decreases slightly with increasing n_0 and increases slightly with v_d.

Fig. 2 shows the amplification characteristics of m.e.l.w.s by interaction with carrier waves when the diffusion phenomena are neglected. The amplification occurs when the drift velocity exceeds the phase velocity of m.e.l.w.s in common with other elastic-wave amplifiers,[6-8] i.e. when $v_d/v > 1$, we have $\alpha > 0$. It is also seen that the velocity ratio v_d/v at which the maximum gain occurs increases with increasing n_0. When diffusion in the semiconductor is neglected, the maximum gain at the optimum velocity ratio is affected very little by the carrier concentration.

When the diffusion phenomena in the semiconductor are taken into account, the amplification characteristics of m.e.l.w.s change as shown in Fig. 3. Comparing Fig. 3 with Fig. 2, we conclude that diffusion considerably reduces the amplification. It is seen that at values of velocity ratio as in Fig. 3 there is an optimum value of the carrier concentration n_0 for the amplification. The maximum gain will occur at higher values of the velocity ratio than those shown here. It is seen that the curve for $n_0 = 10^{13}$ cm^{-3} shows such a tendency.

Conclusion: The amplification characteristics of m.e.l.w.s by interaction with carrier waves have been reported here using numerical calculations for a system that consists of zinc oxide, gallium-y.i.g. and germanium. The results are similar to those of Bleustein-Gulyaev waves.[8] We note, however, that the delay of these m.e.l.w.s is unidirectional and magnetically tunable, since the coupling between m.s.s.w.s and piezoelectric Love waves depends on the applied magnetic field.

YOSHIAKI IKUZAWA
NION SOCK CHANG
YUKITO MATSUO

Institute of Scientific and Industrial Research
Osaka University
Yamadakami, Suita, Osaka 565, Japan

24th October 1978

References

1 PAREKH, J. P.: 'Magnetoelastic surface wave in ferrites', *Electron. Lett.*, 1969, **5**, pp. 322-323
2 MATTHEWS, H., and VAN DE VAART, H.: 'Magnetoelastic Love waves', *Appl. Phys. Lett.*, 1969, **15**, pp. 373-375
3 PAREKH, J. P.: 'Influence of surface metallisation on magnetoelastic surface wave', *Electron. Lett.*, 1970, **6**, pp. 47-48
4 VAN DE VAART, H.: 'Magnetoelastic Love-wave propagation in metal-coated layered substrates', *J. Appl. Phys.*, 1971, **42**, pp. 5305-5312
5 IKUZAWA, Y., CHANG, N. S., and MATSUO, Y.: 'Propagation characteristics of magnetoelastic Love-waves coupled with carrier waves in a piezoelectric-magnetic-semiconductor composite system'. *Trans. Inst. Electron. & Commun. Eng. Japan*, 1978, **J61-B**, pp. 677-678 (in Japanese)
6 WHITE, D. L.: 'Amplification of ultrasonic waves in piezoelectric semiconductor', *J. Appl. Phys.*, 1962, **33**, pp. 2547-2554
7 KINO, G. S., and REEDER, T. M.: 'A normal mode theory for the Rayleigh wave amplifier', *IEEE Trans.*, 1971, **ED-18**, pp. 909-920
8 SOLUCH, W.: 'Theory of amplification of Bleustein-Gulyaev waves in tetragonal and hexagonal crystals', *ibid.*, 1977, **SU-24**, pp. 43-48

0013-5194/79/010017-02$1.50/0

NOISE RELATIONS OF INVERSE ACTIVE NETWORKS AND COMPLEMENTARY NETWORKS

Indexing terms: Active networks, Noise

A direct relation is derived to calculate the noise of an inverse active network from the noise of its pair. A similar relation for complementary networks is also derived. Applications of these relations are given.

Noise of inverse active networks: If $\bar{v}_o^2$ and $\bar{v}_{o_I}^2$ are the output noise densities of a network N_1 and of its active inverse

respectively, then

$$\bar{v}_{o_I}^2 = \bar{v}_o^2/|G|^2$$

where G is the gain between the output and the input of the network N_1.

Proof: A linear active 2-port network N_1 and its inverse active network[1] are shown in Fig. 1. The gain G of the network N_1

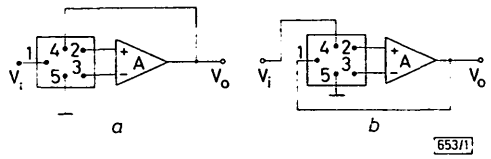

Fig. 1 *Inverse active networks*
a Network N_1
b Inverse of network N_1

can be expressed using Masson's rule in the form

$$G = (t_{12} - t_{13})/(t_{43} - t_{42}) \quad (1)$$

where t_{ij} is the transfer function between ports i and j when all other ports are short circuited and the gain of the operational amplifier is assumed to be infinite.

If a noise source $V_{kk'}$ appears between nodes kk' of network N_1, then the transfer function H_{ko} between the output and the noise source is

$$H_{ko} = (t_{kk'-2} - t_{kk'-3})/(t_{43} - t_{42}) \quad (2)$$

Similarly for the inverse active network;

$$H_{ko_I} = (t_{kk'-2} - t_{kk'-3})/(t_{13} - t_{12}) \quad (3)$$

From eqns. 1–3, it follows that the output noise densities of the pair of inverse active networks are related by

$$\bar{v}_{o_I}^2 = \bar{v}_o^2/|G|^2 \quad (4)$$

Application: Fig. 2 shows two inverse networks, a differentiator N_1 and an integrator.

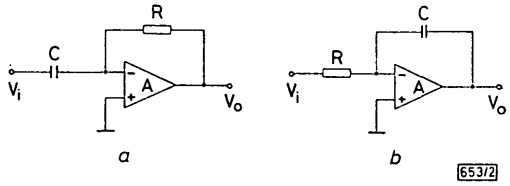

Fig. 2 *Pair of inverse active networks*
a Differentiator N_1
b Miller integrator

The calculated output noise density of the differentiator N_1, which is caused by the thermal noise of the resistance and the different noise sources of the operational amplifier[4] is given by

$$\bar{v}_{o_d}^2 = 4kT[(R + g_{n1} R^2 + r_n)(\omega_0^2/\omega^2) + r_n]\omega^2/\omega_0^2 \quad (5)$$

and the gain of this differentiator is

$$G^2 = \omega^2/\omega_0^2 \quad (6)$$

Similarly, the output noise density of the integrator shown is

$$\bar{v}_{o_I}^2 = 4kT[(R + g_{n_1} R^2 + r_n)\omega_0^2/\omega^2 + r_n] \quad (7)$$

which is equal to

$$\bar{v}_{o_I}^2 = \bar{v}_{o_d}^2/|G|^2 \quad (8)$$

Noise in complementary networks:

(a) Output and ground as complement: The output noise densities $\bar{v}_o^2$ and $\bar{v}_{oc}^2$ of two complementary networks are equal.

Proof: A 2-port network N_1 and its complementary network are shown in Fig. 3.[2] The transfer function between a noise voltage source $v_{kk'}$, appearing between nodes k and k' of network N_1, and the output is

$$H_{kk'-0} = (t_{kk'-2} - t_{kk'-3})/(t_{13} - t_{12}) \quad (9)$$

where t_{ij} is the transfer function between ports i and j when all other ports are short circuited and the gain of the operational amplifier is assumed to be infinite.

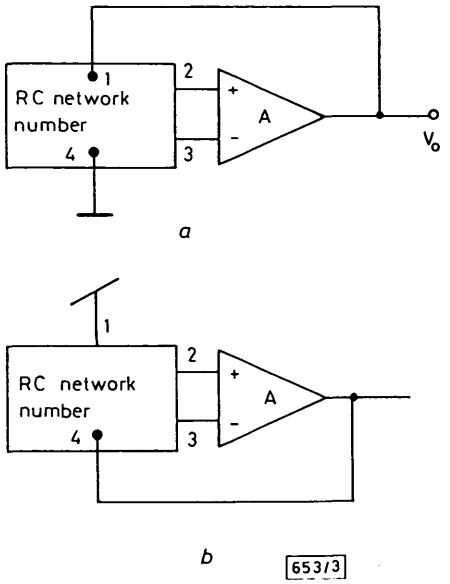

Fig. 3 *Complementary network*
a Network N_1
b Complementary network

Similarly, for the complementary network

$$H_{c_{kk'-0}} = (t_{kk'-2} - t_{kk'-3})/(t_{43} - t_{42}) \quad (10)$$

For passive RC ungrounded networks, it can be shown that[3]

$$t_{12} + t_{42} = 1 \quad (11)$$

and

$$t_{13} + t_{43} = 1 \quad (12)$$

Hence, from eqns. 9–12, the output noise densities $\bar{v}_o^2$ and $\bar{v}_{oc}^2$ are equal.

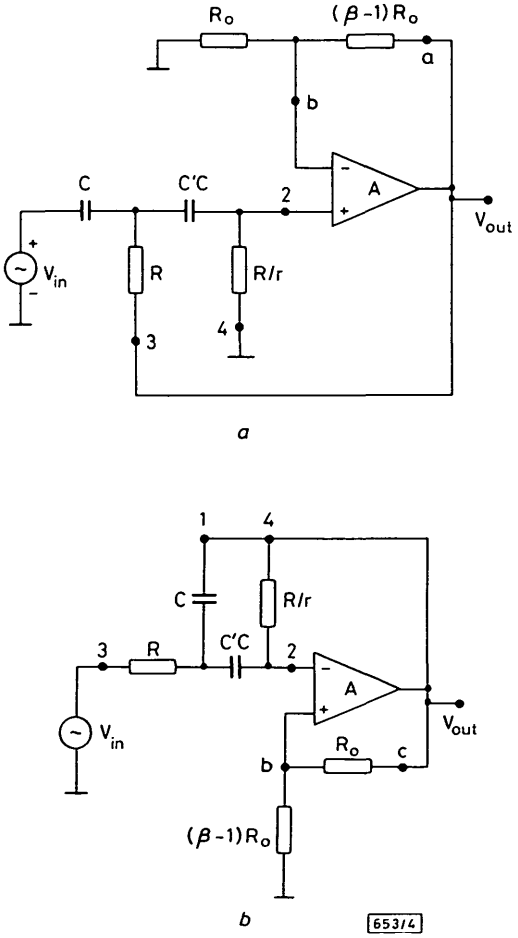

Fig. 4 *Pair of complementary networks*
a H.P. network
b Delyannis section

Application: Fig. 4 shows an h.p. network and its complementary (O/G). The expression of the total output noise density of these networks is lengthy because of the numerous noise sources incorporated in these circuits. However, we consider only a single element and calculate the output noise due to this element. The output noise density due to the resistance R in both circuits with all other noise sources being either short circuited or open circuited is given by

$$\bar{v}_{o_R}^2 = 4kTR\beta(c'/r)|H_{BP}|^2 = \bar{v}_{o_{Rc}}^2 \quad (13)$$

where $|H_{BP}|^2 = \omega^4/\omega_0^4$

(b) Input and ground as complement:[3] Assuming that the input source is an ideal voltage source, the noise spectral densities of the complementary networks are identical.

Conclusion: Noise relations between networks and their inverse active and complementary networks have been derived. These relations facilitate noise analysis of complicated circuits once its inverse active or its complementary noise calculations are carried out since these networks were proved to be related by a very simple relationship.

M. NOMAIR
Y. Z. BAHNAS
A. M. SOLIMAN

Electronics Department
Faculty of Engineering
Cairo University, Egypt

15th November 1978

References

1 RATHORE, T. S.: 'Inverse active networks', *Electron. Lett.*, 1977, **13**, pp. 303–304
2 MOSCHYTZ, G. S., and HORN, P.: 'Optimising two commonly used active filter building blocks using the complementary transformation', *IEE J. Electron. Circuits & Syst.*, 1977, **1**, pp. 125–132
3 HILBERMAN, DAN: 'Input and ground as complements in active filters', *IEEE Trans.*, 1973, **CT-20**, pp. 540–547
4 TROFIMENKOFF, F. N., TRELEAVEN, D. H., and BRUTON, L. T.: 'Noise performance of RC active quadratic filter sections', *ibid.*, 1973, **CT-20**, pp. 524–532

0013–5194/79/010018–03$1.50/0

DISCHARGE MECHANISMS IN FLOATING-GATE E.P.R.O.M. CELLS

Indexing terms: Field-effect integrated circuits, Integrated memory circuits, Read-only storage

Measurements of charge loss from floating-gate e.p.r.o.m. cells have been made at low temperatures by applying terminal voltages to accelerate the discharge. The results strongly suggest that the operative mechanism is electronic tunnelling, implying that it is not possible to make a simple Arrhenius extrapolation from high-temperature storage experiments to service conditions.

The floating-gate, two-layer polysilicon, n-channel m.o.s. transistor is widely used as a nonvolatile memory element. When making long-term data-retention predictions from accelerated life tests it is important to know the mechanism of charge loss from the floating gate. The usual conduction mechanism for thermally grown silicon dioxide is Fowler-Nordheim tunnelling of electrons from the cathode.[1] Frohman-Bentchkowsky, however, in a paper[2] dealing with the similar p-channel f.a.m.o.s. transistor, has asserted that electron transport through the oxide is not capable of predicting currents high enough to account for the experimentally observed charge decay rates. Instead, he has invoked two different mechanisms to account for the time dependence of the discharge. He considers that the rapid (< 100 s) initial charge loss is due to back-tunnelling of electrons from shallow traps at the silicon-substrate/first-thermal-oxide interface and that subsequently a slow hole-trapping mechanism, under the influence of the negative bias produced by the stored charge, gives a logarithmic time dependence. Discharge measurements are reported here that lead to the belief that electronic conduction through the oxide is, after all, the operative mechanism.

To measure the discharge of an e.p.r.o.m. cell in a reasonable time, the discharge rate may be increased either by the use of elevated temperature[2, 3] or by increasing the electric field in the oxide by applying terminal voltages. This second method has been used here, allowing measurements to be made at room temperature and below. In Fig. 1 the floating gate of the e.p.r.o.m. cell has been negatively charged by writing with large positive top-gate and drain voltages. The normalised discharge curves are then shown for a range of top-gate voltages (V_{G2}). The cell was u.v. erased and reprogrammed to the same initial charge level between each discharge cycle.

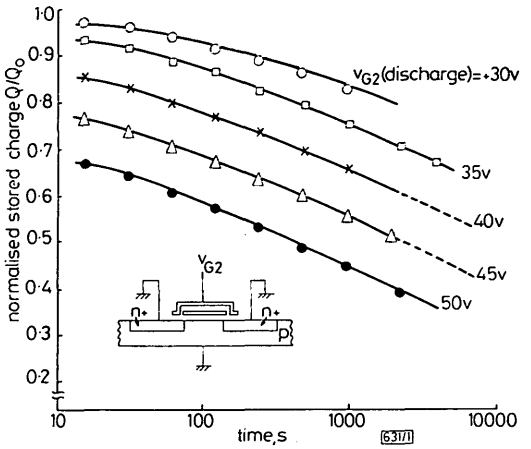

Fig. 1 *Normalised room-temperature decay of stored charge with the top gate voltage as a parameter*
$Q_0/q \approx 2 \times 10^{12}$ cm^{-2}

The charge Q was calculated by assuming the change in the cell threshold voltage to be due entirely to charge stored on the floating gate. The results were repeatable, confirming that the erasure/programming had negligible effect. The discharge is enhanced by the positive top-gate voltage. As the net field at the substrate/oxide interface is strongly positive (from oxide to substrate), this behaviour is exactly opposite to that expected for the slow hole-trapping mechanism. The discharge is similarly enhanced by increasingly negative top-gate voltages, showing that the discharge is principally determined by the magnitude of the oxide field.

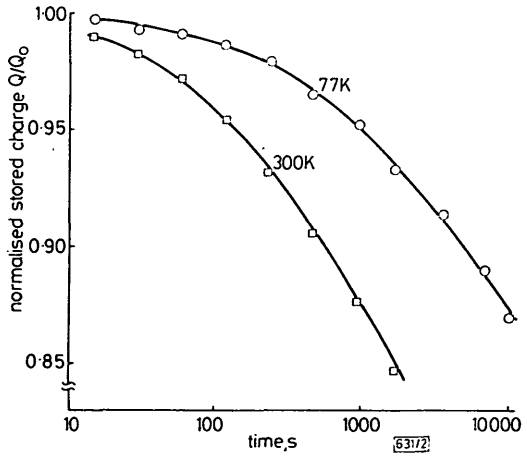

Fig. 2 *Normalised decay of stored charge at room temperature and 77 K*
Top gate voltage = +30 V, $Q_0/q \approx 2 \times 10^{12}$ cm^{-2}

Further evidence of the inapplicability of the hole trapping theory is given in Fig. 2 where the discharge curves at 77 K and 300 K for $V_{G2} = 30$ V show insufficient difference to account for a process with a 1 eV activation energy. In fact, these results are strongly indicative of Fowler–Nordheim conduction, a process that does not have a simple activation energy but instead has a temperature dependence that increases with increasing temperature. Alexander[3] has recently measured the charge-retention properties of n-channel e.p.r.o.m.s during high-temperature (200–300° C) bakes and